Analysis and Simulation of PID-PSS design for power system stability improvement

Mehdi Mahdavian[1], Ghazanfar Shahgholian[2], Mohammadreza Janghorbani[3], Saeed Farazpey[1], Manijeh Azadeh[1]
[1]Department of Electrical Engineering, Naein Branch, Islamic Azad University
Naein, Isfahan, Iran, meh_mahdavian@yahoo.com
[2]Department of Electrical Engineering, Najafabad Branch, Islamic Azad University
Najafabad, Isfahan, Iran, shahgholian@iaun.ac.ir
[3]Young Researchers and Elite Club, Central Tehran Branch, Islamic Azad University, Tehran, Iran

***Abstract*—Power system dynamic performance is improved by the damping of system oscillations. Power system stabilizers are added to excitation systems to enhance the damping during low frequency oscillations. In this paper, the structure of a power system stabilizer based on PID controller for system stability enhancement is presented. The voltage regulator excitation system is assumed to be equipped with IEEE type-DC1exciter model. The application of the controller is investigated by means of simulation studies on a single machine infinite bus power system. For the system without any PSS and the system with conventional PSS (CPSS) and proportional-integral-derivative PSS (PID-PSS), the system responses for three different conditions were obtained using equations linear simulation. Eigenvalues analysis is used for comparison. The simulation results show that, the controller is effective in improving steady state and dynamic system performances regardless of the system operating conditions.**

Keywords—power system stabilizer; modelling; small signal stability; eigenvalues analysis.

I. INTRODUCTION

Modern power systems are complex, nonlinear and often exhibit electromechanical oscillations due to inadequate system damping. Power systems continuously experience changes during abnormal operating conditions due to variations in generation or load and a wide range of disturbances. Power system stability improvements have been considered an important problem for secure system operation over many years [1-4]. Because of the complexity of the network evolved from the interconnected large transmission systems and heavy generations, the use of the power system stabilizer (PSS) has become common by the utilities today [5,6]. PSS is the most usual way to enhance the dynamic stability of power systems. The PSS is used to generate supplementary control signals for the excitation system in order to dampen the low frequency oscillations, increase the system positive damping and improve the steady-state stability margin. Generally, PSS control design methodologies can be categorized as (a) classical method, (b) adaptive and variable structure methods, (c) robust control approaches, (d) intelligent techniques and (e) digital control schemes [7-10]. A number of studies have been performed about the PSS parameters design and its applications to improve the dynamic stability of power systems [11-14].

978-1-4673-9749-0/16/$31.00 ©2016 IEEE

A space recursive least square (SPARLS) algorithm developed for tuning of PSS parameters on SMIB power system based PID is proposed in [15] to meet the vulnerable conditions. A robust control strategy to synthesis of robust PID based power system stabilizers show in [16], which a real-time experiment for longitudinal four machine infinite-bus system to illustrate to find an optimal gain vector via an H_1 static feedback control. The PSS design based on optimal fuzzy PID is considered for single-machine power systems in [17] to control low-frequency oscillation on power systems. A robust PID-based PSS to properly function over a wide range of operating conditions is proposed in [18]. The optimal design of settings of PSS parameters that shift the system eigenvalues associated with the electromechanical modes to the left in the s-plane using evolutionary programming optimization technique is presented in [19]. A step-by-step coordinated design procedure for PSS and automatic voltage regulator in a strongly coupled system is presented in [20]. A self-tuning PID-PSS base on a decentralized structure for improving the dynamic stability of a multi-machine power system over a wide range of operating conditions is presented in [21], which only local measurements within each generating units are required for the adaptation process.

The objective of this paper is to investigate the effects of PSS based PID controllers on power system electromechanical oscillation damping. The synchronous generator is represented by the third-order model. The parameters of PSS are determined based on a linearized model of the power system around a nominal operating point where they can provided good performance. The effectiveness of the proposed PSS in increasing the damping of low-frequency oscillation is demonstrated in a single-machine infinite-bus (SMIB) for different operating conditions of the power system.

II. POWER SYSTEM DYNAMIC MODEL

The SMIB power system configuration shown in Fig. 1 with IEEE type-DC1 excitation system is considered for this study. Here A, B, C and D are equivalent parameters looking from the machine terminal to the external system and therefore reflect operating conditions of the external system. It consist the shunt load in bus T and impedance of the transmission line. E_F and U_R are the electrical field output voltage and reference voltage. U_T and U_B are the terminal voltage and infinite-bus voltage.

A. Synchronous Machine

During low frequency oscillations damper windings can be ignored in the model of the power system.

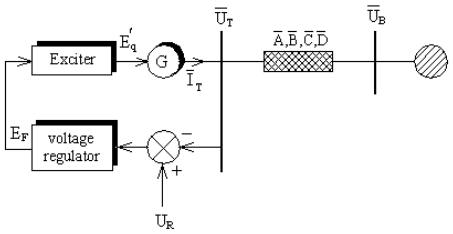

Fig. 1. Single-Machine Infinite-Bus Power System [22]

The synchronous machine model (1,0) used in this paper is a three-order model in the d- and q-axis by neglecting damper windings. The non-linear dynamic model of the generator is given by [23]:

$$\frac{d}{dt}\delta = \omega_b\,\omega_r \tag{1}$$

$$\frac{d}{dt}\omega_r = \frac{1}{J_M}(T_M - T_E) \tag{2}$$

$$\frac{d}{dt}E_q^{'} = \frac{1}{T_{do}^{'}}[E_F - E_q^{'} + (X_d^{'} - X_d)\,i_d] \tag{3}$$

B. Exciter System

The exciter model used in this study is the standard IEEE type-DC1 exciter. The exciter transfer function between the electrical field voltage deviation (ΔE_F) and the error voltage deviation (ΔU_E) of the excitation system as shown in Fig. 2 is given by [24]:

$$G_V(s) = \frac{\Delta E_F(s)}{\Delta U_E(s)} = \frac{G_U(s)\,G_A(s)}{1 + G_S(s)\,G_U(s)\,G_A(s)} \tag{4}$$

where $G_A(s)$, $G_S(s)$ and $G_U(s)$ are transfer function of the voltage regulator system, excitation system stabilizers and saturation. U_E is the error voltage. K_A, K_E and K_S are gains and T_A, T_E and T_S are time constants of the system exciter. Bode plot of the exciter for two different cases include IEEE Type-DC1 exciter system with transfer function $G_V(s)$ and IEEE Type-ST1 exciter system with transfer function $G_A(s)$ are shown in Fig. 3.

C. Synchronous and Damping Torque

The change in the electrical torque deviation can be expressed in terms of reference voltage and rotor angle deviations:

$$\Delta T_E(s) = K_1\Delta\delta + K_2\Delta E_q^{'}(s) =$$

$$K_1\Delta\delta + \underbrace{\frac{-K_2 G_F(s)[K_4 + K_5 G_V(s)]}{1 + K_6 G_F(s)\,G_V(s)}}_{H_Q(s)}\Delta\delta$$

$$+ \underbrace{\frac{K_2 G_F(s)\,G_V(s)}{1 + K_6 G_F(s)\,G_V(s)}}_{G_E(s)}\Delta U_R(s) \tag{5}$$

where $H_Q(s)$ is the control transfer function (between the electrical output torque and load angle) and $G_E(s)$ is the electrical loop transfer function (between exciter input and the output electrical torque). The synchronous torque (T_s) and damping torque (T_d) coefficients are defined as:

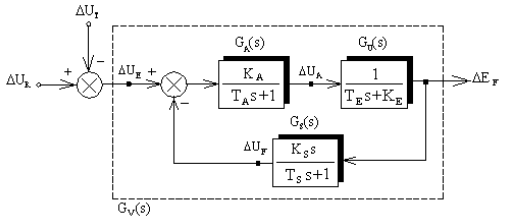

Fig. 2. IEEE type-DC1 excitation system [25]

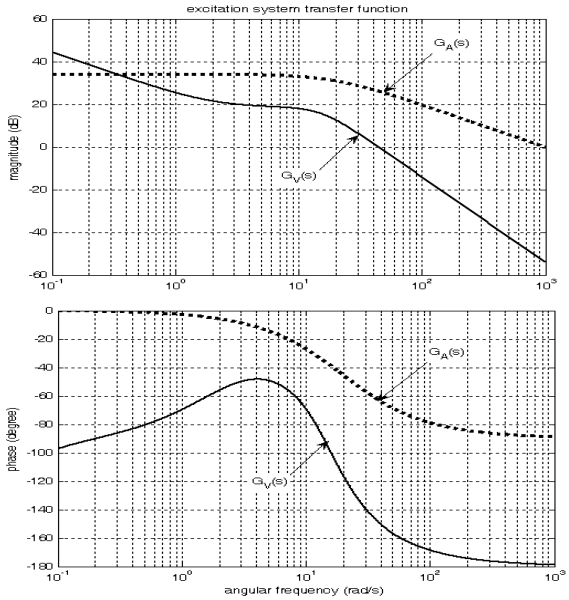

Fig. 3. Bode plot of transfer function $G_V(s)$

$$T_s(\omega) = \mathrm{Re}[H_Q(j\omega)] + K_1 \tag{6}$$

$$T_d(\omega) = \frac{\omega_b}{\omega}\,\mathrm{Im}[H_Q(j\omega)] \tag{7}$$

They are sensitive to power system parameters, synchronous generator operating conditions, and excitation control system parameters.

D. Conventional Lead-Lag PSS

Electromechanical oscillations of power system are damped by compensator as shown in Fig. 4. It consists of an amplifier block of gain constant K_C, a block having a washout time constant T_W and lead-lag compensators with time constants T_D and T_G. The gain and the lead-lag compensator time constants are to be selected for optimal performance over a wide range of operating conditions. The transfer function of CPSS is given by [26]:

$$G_L(s) = K_C\,\frac{T_W s}{1 + T_W s}\left(\frac{1 + T_D s}{1 + T_G s}\right)^2 \tag{8}$$

Fig. 5 show the phase frequency response characteristics of CPSS (T_G=0.05) according to the variation of T_D.

E. PID-PSS

A PID controller is commonly used by industrial utilities. It can be represented in transfer function form as [27,28]:

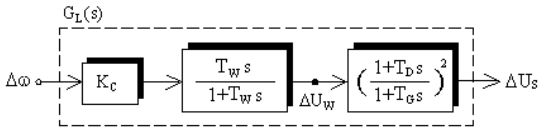

Fig. 4. Block diagram of conventional power system stabilizer (CPSS)

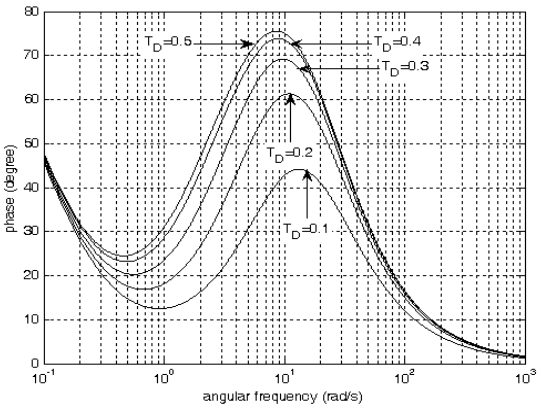

Fig. 5. Phase frequency response characteristics of the CPSS

$$G_C(s) = K_P + \frac{K_I}{s} + K_D s \tag{9}$$

where represents the proportional gain, represents the integral gain, and represents the derivative gain, respectively K_P, K_I and K_D. The phase angle diagram of the PID controllers for different values of gains are shown in Fig. 6. The PID-PSS as shown in Fig. 7 with rotor deviation as input have the following transfer function:

$$G_P(s) = K_G(\frac{T_W}{1+T_W s})(K_P + \frac{K_I}{s} + K_D s) \tag{10}$$

The corresponding magnitude and phase characteristic are given by:

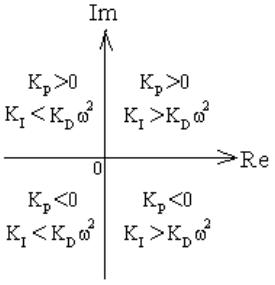

Fig. 6. Phase angle diagram of the PID controller

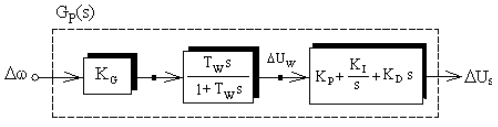

Fig. 7. Block diagram of PID power system stabilizer (PID-PSS)

$$M(\omega) = K_G \frac{T_W}{\sqrt{1+(T_W\omega)^2}} \sqrt{K_P^2 + (K_D\omega - \frac{K_I}{\omega})^2} \tag{11}$$

$$\theta_P(\omega) = 180 + tg^{-1}\frac{[K_P - T_W(K_I - K_D\omega^2)]\omega}{K_I + (K_P T_W - K_D)\omega^2} \tag{12}$$

F. Transfer FUnction

The transfer function block diagram representing the small signal stability model can be simplified as shown in Fig. 8. The linearized model of a SMIB power system has six eigenvalues. Therefore, the characteristic equation of the open loop SMIB power system is given by:

$$\Delta_T(s) = s^6 + g_5 s^5 + g_4 s^4 + g_3 s^3 + g_2 s^2 + g_1 s + g_0 \tag{13}$$

By varying the operating point, the coefficient parameter values g_0 through g_5 also vary. The open loop transfer function from $\Delta\omega_r$ to ΔU_R, which plays an important role in the closed loop design, is given by:

$$H_{SU}(s) = \frac{\Delta\omega_r(s)}{\Delta U_R(s)} = \frac{s\,G_M(s)\,G_E(s)}{s + \omega_b G_M(s)[K_1 + H_Q(s)]} \tag{14}$$

$$H_{SU}(s) = \frac{\Delta\omega_r(s)}{\Delta U_R(s)} = \frac{1}{\Delta_T(s)}(\underbrace{-\frac{K_2 K_A}{J_M T_{do}^{'} T_E T_A}}_{K_O}) s(s + \frac{1}{T_S}) \tag{15}$$

III. SMALL SIGNAL MODEL

Small signal stability is best analyzed by linearizing the system differential equations about equilibrium operating point. Fig. 9 display a block diagram of a SMIB comprehensive model. The linearized model parameters K_1 to K_6 vary with operating point (P_{EO},Q_{EO},U_{TO}) with the exception of K_3. The synchronous machine model along with the associated regulating devices thus becomes an eight-order model for PID-PSS and nine-order model for CPSS. When the PSS is used in SMIB power system, the close loop transfer function can be expressed as follows:

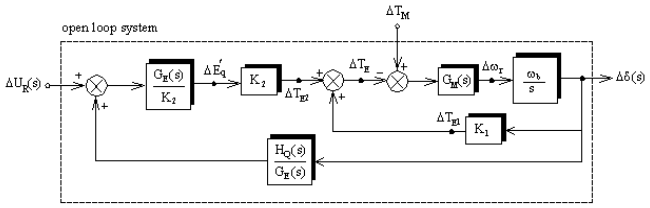

Fig. 8. Transfer function block diagram of SMIB power system

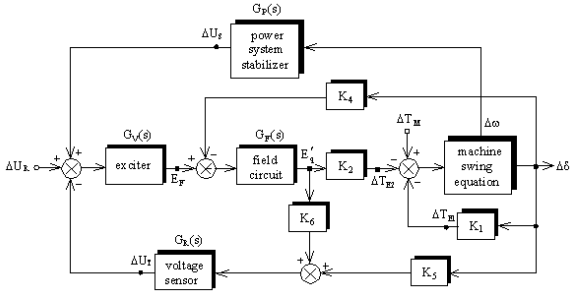

Fig. 9. Single-machine infinite-bus model

$$H_{RU}(s)=\frac{\Delta\omega_r(s)}{\Delta U_R(s)}=\frac{H_{SU}(s)}{1-H_{SU}(s)G_P(s)} \quad (16)$$

By using $H_{RU}(s)$, the characteristic equation of the close loop SMIB power system equipped with PID-PSS is given by:

$$\Delta_{HP}(s)=s(s^7+h_6s^6+h_5s^5+h_4s^4+h_3s^3+h_2s^2+h_1s+h_0) \quad (17)$$

where the coefficients h_0 through h_6 are given by:

$$h_6=g_5+\frac{1}{T_W} \quad (18)$$

$$h_5=g_4+\frac{g_5}{T_W} \quad (19)$$

$$h_4=g_3+\frac{g_4}{T_W}-K_OK_GK_D \quad (20)$$

$$h_3=g_2+\frac{g_3}{T_W}-\frac{K_OK_G}{T_S}(K_PT_S+K_D) \quad (21)$$

$$h_2=g_1+\frac{g_2}{T_W}-\frac{K_OK_G}{T_S}(K_P+K_IT_S) \quad (22)$$

$$h_1=g_0+\frac{g_1}{T_W}-\frac{K_OK_GK_I}{T_S} \quad (23)$$

$$h_0=\frac{g_0}{T_W} \quad (24)$$

To increase the system damping, the eigenvalue-based objective function is considered as follows:

$$J=\max[\mathrm{Real}(\lambda_i)] \quad (25)$$

where λ_i is the ith electromechanical mode eigenvalue. In the optimization process, it is aimed to minimize J in order to shift the poorly damped eigenvalues to the left in s-plane.

IV. Simulation Results

The nominal operating conditions and system parameters are given in Table I. The optimal gains of the PI-PSS [29] and PID-PSS are shown in Table II. The K_1 value under normal load operation is 1.4462, therefore the electromechanical mode natural angular frequency (ω_n) is 10.7448 rad/s. The system eigenvalues with and without the proposed stabilizer for three different conditions are given in Tables III, IV and V.

It shows the electrometrical mode eigenvalue with its damping ratio for the open loop system.

TABLE I. System parameters and operation data

Generator	J_M=4.74, X_d=1.7, X'_d=0.254 X_q=1.64, T'_{do}=5.9 s, f=60 Hz
IEEE type-ST1 excitation system	K_A=400, T_A=0.05 s
IEEE type-DC1 excitation system	K_A=400, T_A=0.05 s, K_E=-0.17 T_E=0.95 s, K_S=0.025, T_S=1 s
Normal load operation	P_{EO}=1, Q_{EO}=0.62, U_{TO}=1.172
Heavy load operation	P_{EO}=1.4, Q_{EO}=1.1, U_{TO}=1.172
Light load operation	P_{EO}=0.3, Q_{EO}=0.1, U_{TO}=1.172
Transmission line reactance	R_E=0.02, X_E=0.4
Undamped natural angular frequency	ω_n=10.7448 rad/s

TABLE II. System parameters and operation data

PSS	Parameters
PID-PSS	T_W=0.1149 s, K_G=20, K_P=-0.6871, K_I=-7.9162, K_D=0.0688
PI-PSS	T_W=0.1s, K_G=10, K_P=-1.075, K_I=-15.528

TABLE III. System eigenvalues for normal load operation

Without PSS	With PID-PSS
-0.2350±j10.7852	-2.7130±j10.8539
-8.1340±j8.9851	-7.8708±j3.6719
-3.0830	-3.7595±j6.3345
-1.5520	-1.3896
---	0
---	---

TABLE IV. System eigenvalues for heavy load operation

Without PSS	With PID-PSS
-0.301±j10.1575	-4.0471±j10.6330
-7.7731±j9.3124	-1.6751±j7.2454
-4.3901	-8.6648±j3.2515
-1.3762	-1.3020
---	0
---	---

TABLE V. System eigenvalues for light load operation

Without PSS	With PID-PSS
-0.3712±j8.7370	-1.4517±j6.8385
-7.6502±j8.6151	-5.1094±j8.9276
-4.0019	-7.8385±j2.7312
-1.3282	-1.2769
---	0
---	---

Also, it is observed that the electromechanical mode for the open-loop system, which are characterized by the eigenvalues -0.2350±j 10.7852 for normal operating, -1.8391±j7.4204 for heavy load and -1.6506±j 7.3189 for light load, are poorly damped. It is clear that the system stability is greatly enhanced with the proposed stabilizers. The system response without applying any PSS is more oscillatory in heavy load condition. The dynamic behavior response of the SMIB power system as the function of the loading is shown in Figures 10 and 11. In all the figures, the response with normal load is shown with dotted line with legend NL, the response with light load is shown with dashed lines with legend LL and the response with heavy load is shown with solid line with legend HL respectively. Table VI shows the summary of the system dynamic characteristics such as settling time (t_s), peak time (t_p) and percent overshoot (M_P). The system responses are shown in Fig. 12. In the figures, the response without any PSS is shown with dotted line with legend NP, the response with conventionally designed power system stabilizer is shown with dashed lines with legend CP and the response with proposed PID-PSS are shown with solid line with legend PP respectively. As is observed from the figure, the system response for the PID-PSS is optimum in different condition. The CPSS has a well-damped response and a lower peak offshoot in all cases investigated. The damping ratio of the electrometrical mode eigenvalue for different loading of the power system without PSS and PSS are shown in Table VII. In Fig. 13 trajectory of the load angle of the generator is shown. It can be seen that CPSS damping is bigger than PID-PSS and PI-PSS damping. The PSS output response to step

mechanical torque change is shown in Fig. 14. As it seems PID-PSS and PI-PSS outputs are better than the CPSS output.

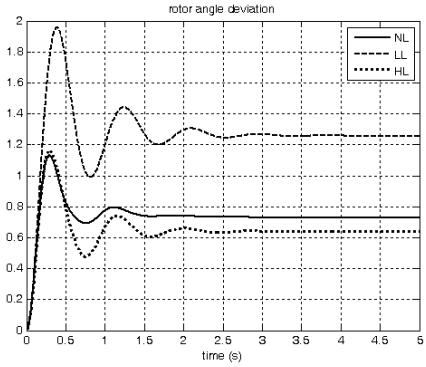

(a) with CPSS

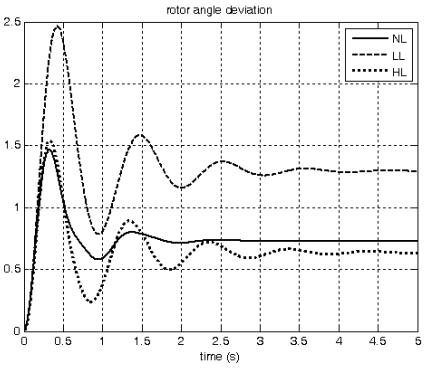

(b) with PID-PSS

Fig. 10. System rotor angle deviation response for different loading

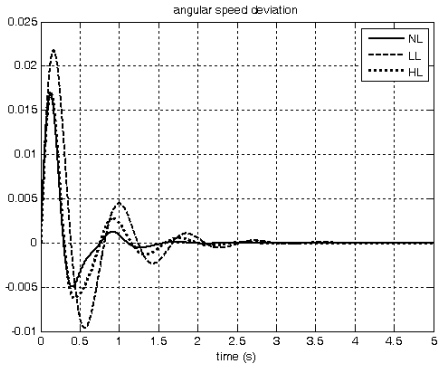

(a) with CPSS

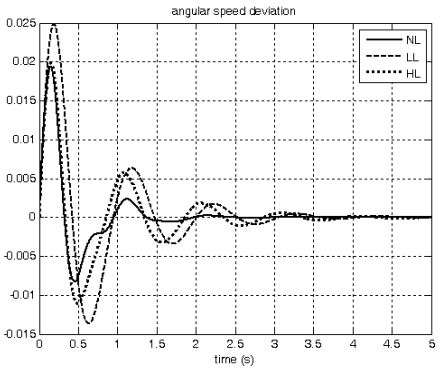

(b) with PID-PSS

Fig. 11. System angular speed deviation response for different loading

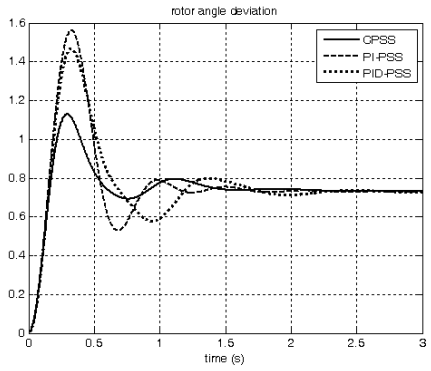

(a) rotor angle deviation

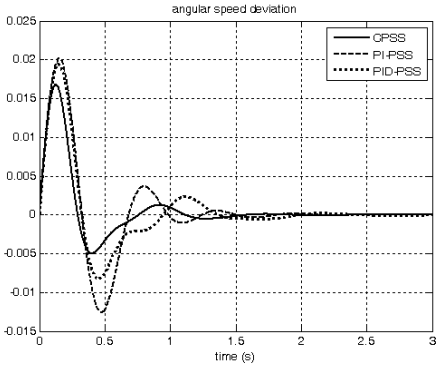

(b) rotor speed deviation

Fig. 12. System dynamic behaviour response with PSS in normal load

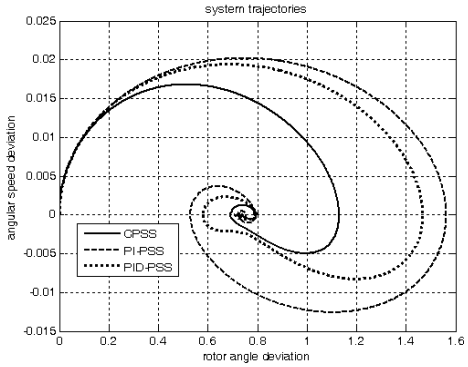

Fig. 13. System trajectories in the δ-ω phase-plane of the generator

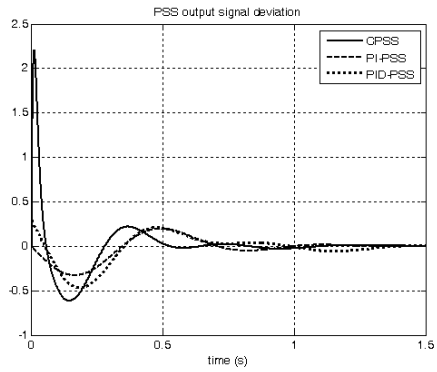

Fig. 14. PSS output response to a step mechanical torque change

TABLE VI. SYSTEM DYNAMIC CHARACTERISTICS

Loading	With PI-PSS			With PID-PSS		
	t_s	t_p	M_P%	t_s	t_p	M_P%
Normal loading	1.7 s	3 s	55.21	1.50 s	0.32 s	101.68
Heavy loading	2.5 s	0.3	82.28	3.50 s	0.33 s	142.81
Light loading	3 s	0.4 s	55.85	3.54 s	0.42 s	90.95

TABLE VII. DAMPING RATIO

Loading	Without PSS	PI-PSS	PID-PSS
Normal loading	0.0218	0.2787	0.2425
Heavy loading	0.0030	0.2406	0.2253
Light loading	0.0424	0.2200	0.2077

V. CONCLUSIONS

Power system stabilizer is the most usual way to mitigate power system electromechanical oscillations. A comparison between three different power system stabilizers (CPSS, PI-PSS and PID-PSS) has been carried out on a SMIB power system. Time domain simulations of the system with PID-PSS presented a good speed deviation and change in rotor angle response at different type of loading condition. Simulation results and eigenvalues analysis prove that the CPSS can give adequate performance, although the system-order with CPSS is 9 but the system-order with PID-PSS is 8.

REFERENCES

[1] Gh. Shahgholian, A. Movahedi, J. Faiz, "Coordinated design of TCSC and PSS controllers using VURPSO and genetic algorithms for multi-machine power system stability", Int. J. of Control, Automation, and Systems, Vol. 13, No. 2, pp. 398-409, April 2015.

[2] R.K. Khadanga, J.K. Satapathy, "Time delay approach for PSS and SSSC based coordinated controller design using hybrid PSO–GSA algorithm", Int. J. of Elec. Pow. and Ene. Sys., Vol. 71, pp. 262–273, 2015.

[3] M. Fooladgar, E. Rok-Rok, B. Fani, Gh. Shahgholian, Evaluation of the trajectory sensitivity analysis of the DFIG control parameters in response to changes in wind speed and the line impedance connection to the grid DFIG", J. of Intelligent Procedures in Electrical Technology, Vol. 5, No. 20, pp. 37-54, winter 2015 (in Persian).

[4] G. Guraala, I. Sen, "Power system stabilizers design for interconnected power systems", IEEE Trans. on Pow. Systems, Vol. 25, No. 2, pp. 1042-1051, May 2010.

[5] Gh. Shahgholian, "Review of power system stabilizer: Application, modeling, analysis and control strategy", Int. J. on Technical and Physical Problems of Engineering, Vol. 5, No. 3, pp. 41-52, Sep. 2013.

[6] M. Gitizadeh, M. Kalantar, "Optimum allocation of FACTS devices in fars regional electric network using genetic algorithm based goal attainment", J. of Zhejiang University SCIENCE A, Vol. 10, No. 4, pp. 478-487, 2009.

[7] J. I. Corcau, E. Stoenescu, "Fuzzy logic controller as a power system stabilizer", Int. J. of Circuits, Systems and Signal Processing, Vol.1, No.3, pp.266-272, 2007.

[8] V. Keumarsi, M. Simab, Gh. Shahgholian, "An integrated approach for optimal placement and tuning of power system stabilizer in multi-machine systems", Int. J. of Elec. Pow. and Ene. Sys., Vol. 63, pp. 132-139, Dec. 2014.

[9] V. Mukherjee, S.P. Ghoshal, "Comparison of intelligent fuzzy based AGC coordinated PID controlled and PSS controlled AVR system", Int. J. of Elec. Pow. and Ene. Sys., Vol. 29, No. 9, pp.679-689, Nov. 2007.

[10] Gh. Shahgholian, A. Rajabi, B. Karimi, "Analysis and design of PSS for multi-machine power system based on sliding mode control theory", Int. Review of Electrical Engineering, Vol.4, No.2, pp., Oct. 2010.

[11] Gh. Shahgholian, A. Movahedi, "Coordinated design of thyristor controlled series capacitor and power system stabilizer controllers using velocity update relaxation particle swarm optimization for two-machine power system stability", Revue Roumaine Des Sciences Techniques, Vol. 59, No. 3, pp. 291-301, 2014.

[12] M.A. Mahmud, H.R. Pota, M. Aldeen, M.J. Hossain, "Partial feedback linearizing excitation controller for multimachine power systems to improve transient stability", IEEE Trans. on Pow. Systems, Vol. 29, No. 2, pp. 561-571, March 2014.

[13] Z. Jiang, "Design of a nonlinear power system stabilizer using synergetic control theory", Electrical Pow. Systems Research, Vol. 79, No. 6, pp. 855-862, June 2009.

[14] M.N. Anwar, S. Pan, "A frequency domain design of PID controller for an AVR system", J. of Zhejiang University-SCIENCE C, Vol.15 , No. 4, pp. 293-299, 2014.

[15] A. Ragavendiran, R. Gnanadass, K. Ramakrishnan, "A new SPARLS algorithm for tuning power system stabilizer", Int. J. of Electrical Pow. and Energy Systems, Vol. 68, pp. 327-335, 2015.

[16] H. Bevrani, T. Hiyama, H. Bevrani,"Robust PID based power system stabiliser: Design and real-time implementation", Int. J. of Elec. Pow. and Ene. Sys., No.33, pp.179–188, 2011.

[17] E.A. Hakim, A. Soeprijanto, H.P. Mauridhi, "Fuzzy PID based PSS design using genetic algorithm", Int. J. of Electrical and Electronics Engineering, Vol.4 , pp.345-347, 2010.

[18] M. Solimana, A.L. Elshafei, F. Bendarya,W. Mansoura, " Robust decentralized PID-based power system stabilizer design using an ILMI approach", Elec. Pow. Sys. Res., No.80, pp.1488–1497, 2010.

[19] H. Alkhatib, J. Duveau, "Robust design of power system stabilizers using adaptive genetic algorithms", Wor. Aca. Sci., Eng. and Tec., pp.267-272, Vol.64, 2010.

[20] A. Dysko, W.E. Leithead, J. Reilly, "Enhanced power system stability by coordinated PSS design", IEEE Trans. on Pow. Systems, Vol.25, No.1, pp.413-422, Feb. 2010.

[21] C.J. Wu, Y.Y. Hsu, "Design of self-tuning PID power system stabilizer for multimachine power system", IEEE Trans. on Pow. Systems,Vol. 3, pp. 1059-1064, Aug. 1988.

[22] Gh. Shahgholian, J. Faiz, "The effect of power system stabilizer on small signal stability in single-machine infinite-bus", Int. J. of Electrical and Engineering, Vol. 4, No. 2, pp.45-53, 2010.

[23] Gh. Shahgholian, "Development of state space model and control of the STATCOM for improvement of damping in a single-machine infinite-bus", Int. Review of Electrical Engineering, Vol.4, No.6, pp.1367-1375, Nov./Dec. 2009.

[24] N. Hosaeinzadeh, A. Kalam, "A direct adaptive fuzzy power system stabilizer", IEEE Tran. on Energy Conversion, Vol. 14, No. 4, pp. 1564-1571, Dec. 1999.

[25] K. Bhattacharya, J. Nanda, M.L. Kothari, "Optimization and perf-ormance analysis of conventional power system stabilizers", Int. J. of Elec. Pow. and Ene. Sys., Vol.19, No.7, pp. 449-458, Oct. 1997.

[26] Y.L. Abdel, M.A. Abido, A.H. Mantawy, "Robust tuning of power system stabilizers in multimachine power systems", IEEE Trans. on Pow. Systems, Vol. 15, No. 2, pp. 735-740, May 2000.

[27] Gh. Shahgholian, P. Shafaghi, H. Mahdavi-Nasab, "A comparative analysis and simulation of ALFC in single area system for different turbines", IEEE/ICECT, pp. 50-54, Kuala Lumpur, Malaysia, May 2010.

[28] Gh. Shahgholian, J. Faiz, P. Shafaghi, "Analysis and simulation of speed control for two-mass resonant system", IEEE/ICCEE, pp. 668-672, Dec. 2009.

[29] C.L. Chen, Y.Y. Hsu, "Coordinated tuning of proportional-integral power system stabilizers in multimachine power systems", Electrical Pow. Systems Research, Vol. 11, pp. 71-83, 1986.